doi:10.3969/j.issn.1001-3539.2026.10.006

海藻酸钠/壳聚糖/木质素磺酸钠复合抗菌眼贴水凝胶的制备及性能

王思宇[1],李兢业[2],陈凯[2],薛晶文[2],岑璐莎[1]

[1.浙江中医药大学附属第一医院(浙江省中医院),杭州 310006; 2.浙江科技大学生物与化学工程学院,杭州 310023]

摘要:针对眼贴基材对紫外屏蔽与抗菌性能的协同需求,以木质素磺酸钠(LS)为功能组分,固定海藻酸钠(SA)和壳聚糖(CS)用量均为0.3 g,设置0、50、100、200、400 mg五个LS添加梯度,通过Ca^{2+}离子交联制备了SA/CS/LS复合水凝胶,系统探究LS添加量对水凝胶网络形貌、组分间作用、力学性能、紫外屏蔽和抑菌性能的影响。采用扫描电子显微镜和傅里叶变换红外光谱(FTIR)表征凝胶微观形貌与组分间作用,通过拉伸和加载-卸载测试评价水凝胶力学行为;对LS添加量为0、50、100 mg组的交联前预聚液稀释后,测定紫外-可见透过率及600 nm处光密度(OD_{600}),并分别计算长波紫外线(UVA)和中波紫外线(UVB)波段的表观平均透过率及抑菌率。结果表明,复合水凝胶呈多孔及层状结构,随LS添加量增加,凝胶部分区域网络趋于疏松;FTIR谱带变化与组分间非共价相互作用相符。当LS添加量由50 mg增加到400 mg时,复合水凝胶的拉伸强度由0.513 MPa降至0.233 MPa,耗散能同步降低。LS添加量为100 mg时(SA-CS-LS-2),其预聚液稀释液在UVB和UVA波段的表观平均透过率分别为2.79%和27.57%,均低于0 mg和50 mg组。与大肠杆菌、金黄色葡萄球菌共培养6 h后,LS添加量为50 mg和100 mg组的计算抑菌率均不低于99.99%。综上,LS添加量可调控SA/CS复合水凝胶的微观结构与力学性能,并影响预聚液的紫外屏蔽及抗菌表现;综合各项性能,100 mg LS添加量的配方兼具良好力学性能(拉伸强度0.404 MPa)、优异紫外屏蔽效果与高效抗菌能力,可为抗菌、紫外防护型眼贴水凝胶基材的配方设计提供参考。

关键词:海藻酸钠;壳聚糖;木质素磺酸钠;复合水凝胶;抗菌性能;紫外屏蔽;眼贴基材

中图分类号:TB324;R318.08 **文献标识码**:A **文章编号**:1001-3539(2026)10-0046-08

Preparation and properties of sodium alginate/chitosan/sodium lignosulfonate composite antibacterial hydrogel for periocular patches

WANG Siyu[1], LI Jingye[2], CHEN Kai[2], XUE Jingwen[2], CEN Lusha[1]

[1. The First Affiliated Hospital of Zhejiang Chinese Medical University (Zhejiang Provincial Hospital of Chinese Medicine), Hangzhou 310006, China; 2. School of Biological and Chemical Engineering, Zhejiang University of Science and Technology, Hangzhou 310023, China]

Abstract: To address the demand for UV-protective and antibacterial substrates for periocular patches, sodium alginate (SA)/chitosan (CS)/sodium lignosulfonate (LS) composite hydrogels with the amounts of SA and CS fixed at 0.3 g each were developed via Ca^{2+}-mediated ionic crosslinking, and the effects of LS dosage (0, 50, 100, 200, 400 mg) on their microstructure, interfacial interactions, mechanical properties, UV-shielding capacity, and antibacterial activity were systematically investigated. The morphology and chemical interactions were characterized by scanning electron microscopy and Fourier-transform infrared spectroscopy (FTIR). Tensile and cyclic loading-unloading tests were performed to evaluate the mechanical behavior. After diluting the pre-polymerization solution with 0, 50, 100 mg of LS added, the ultraviolet-visible transmittance and optical density at 600 nm (OD_{600}) were measured, and the apparent average transmittance and antibacterial rate in the long-wave ultraviolet (UVA) and medium-wave ultraviolet (UVB) bands were calculated respectively. The results show that the composite hydrogel has a porous and layered structure. With the

基金项目:2025年国家级大学生创新创业训练计划(202510344059),浙江省康复医学会科研专项基金项目(ZKKY2024018)

通信作者:岑璐莎,博士,副主任医师,硕士生导师,研究方向为中西医结合眼病诊治

收稿日期:2026-08-04

引用格式:王思宇,李兢业,陈凯,等.海藻酸钠/壳聚糖/木质素磺酸钠复合抗菌眼贴水凝胶的制备及性能[J].工程塑料应用,2026,54(10):46-53.
WANG Siyu, LI Jingye, CHEN Kai, et al. Preparation and properties of sodium alginate/chitosan/sodium lignosulfonate composite antibacterial hydrogel for periocular patches [J]. Engineering Plastics Application, 2026, 54(10): 46-53.

increase of LS content, the network in some areas tend to be loose.Changes in FTIR bands are consistent with noncovalent interactions among the components. When the addition amount of LS increases from 50 mg to 400 mg, the tensile strength of the composite hydrogel decreases from 0.513 MPa to 0.233 MPa, and the dissipated energy decreases simultaneously. At 100 mg LS (SA-CS-LS-2), the diluted pre-crosslinking solution shows apparent mean transmittances of 2.79% and 27.57% in the UVB and UVA bands, respectively, both lower than those of the 0 and 50 mg groups. After of co-incubation with Escherichia coli and Staphylococcus aureus for 6 h, the calculated inhibition rates of the groups with 50 mg and 100 mg of LS addition are both not lower than 99.99%. In summary, the addition amount of LS can regulate the microstructure and mechanical properties of SA/CS composite hydrogels, and affect the UV shielding and antibacterial performance of the prepolymer solution. Based on the comprehensive performance, the formula with 100 mg LS addition has good mechanical properties (tensile strength 0.404 MPa), excellent ultraviolet shielding effect and efficient antibacterial ability, which can provide reference for the formulation design of antibacterial and ultraviolet protective eye patch hydrogel substrate.

Keywords : sodium alginate ; chitosan ; sodium lignosulfonate ; composite hydrogel ; antibacterial property ; ultraviolet shielding ; periocular patch substrate

外用眼贴水凝胶需适应眼周皮肤的曲率变化和湿润环境,并兼顾柔软贴合、保水、湿态结构稳定性与生物安全性。天然高分子水凝胶因具有可调的网络结构及复合改性空间,已用于创面护理等研究[1−2]。本文所述眼贴基材面向眼周皮肤外用贴敷,不涉及角膜或结膜直接接触。眼周日光防护也是此类材料的一项设计需求。长波紫外线(UVA)和中波紫外线(UVB)与皮肤光老化及眼部光损伤相关[3−5],因此,在凝胶基体中引入具有紫外吸收能力的组分,有助于拓展眼贴基材的辅助防护功能。材料配方还需兼顾基础力学性能和抑菌表现,避免单一功能增强伴随结构稳定性下降。

近年来,天然高分子凝胶的组分复合和网络调控受到广泛关注[6−7]。海藻酸钠(SA)含羧酸盐基团,可与Ca^{2+}形成离子交联网络;壳聚糖(CS)含氨基和羟基,可参与分子间作用。已有研究通过自修复、三维打印和离子复合等途径改善SA基或SA/CS材料的结构与性能[8−11];互穿网络也用于改善其他高分子凝胶的力学表现[12]。木质素磺酸钠(LS)含磺酸盐基团、酚羟基和芳香结构,具有亲水性和复合改性潜力[13−15]。木质素及其衍生物在复合材料中的紫外吸收与屏蔽作用已有报道[15−18]。此外,CS的抗菌活性[19]及木质素基纳米颗粒的抗菌作用[20]也已有报道。结果表明,LS的功能贡献取决于基体组成及网络状态,需针对具体凝胶体系考察其添加量效应。

近期,Sun等[21]将LS与膨润土引入CS薄膜,改善了其力学与紫外阻隔性能;Van等[22]通过调节CS含量改变SA/卡拉胶复合凝胶的力学、溶胀和抗菌表现;Zhang等[23]已报道Ca^{2+}交联SA/LS凝胶的保水应用。与这些薄膜复合、组分配比或保水研究相比,本文聚焦LS在Ca^{2+}交联SA/CS体系中的添加量效应,联系网络形貌、力学耗散与配方功能筛选。

本研究以SA和CS为基体,以LS为功能组分,采用Ca^{2+}离子交联制备复合水凝胶。围绕LS添加量变化,分析凝胶形貌、组分间作用和力学行为,并结合配液的紫外光谱与600 nm处光密度(OD_{600})计算抑菌结果,讨论LS低添加量区间的力学与功能平衡,为外用眼贴基材的配方设计提供依据。

1 实验部分

1.1 主要原材料

SA:含量90%,上海麦克林生化科技股份有限公司;

CS:脱乙酰度≥95%,分析纯,上海麦克林生化科技股份有限公司;

LS:分析纯,上海阿拉丁生化科技股份有限公司;

无水氯化钙:含量96%,上海麦克林生化科技股份有限公司;

胰酪大豆胨液体培养基(TSB):干粉,上海麦克林生化科技股份有限公司;

去离子水:实验室自制;

大肠杆菌(Escherichia coli CICC 10003)和金黄色葡萄球菌(Staphylococcus aureus CICC 10438)由中国工业微生物菌种保藏管理中心提供。

1.2 主要仪器及设备

加热磁力搅拌器:205D,国药集团化学试剂有限公司;

−80 ℃医用低温保存箱:DW-86L388 J,青岛海尔特种电器有限公司;

冷冻干燥机:SCIENTZ-12N,宁波新芝生物科

技有限公司;

智能电子拉力试验机:TST-01M,济南众测机电设备有限公司;

扫描电子显微镜(SEM):SU1510,日立高新技术(上海)有限公司;

酶标仪:NNR07404,美谷分子仪器(上海)有限公司;

pH 计:PHS-3E,上海仪电科学仪器股份有限公司;

傅里叶变换红外光谱(FTIR)仪:TENSOR-27,德国 Bruker公司;

紫外-可见分光光度计:UV-2600,日本岛津公司。

1.3 试样制备

(1)交联液配制:将 2.5 g 无水氯化钙加入 100 g 去离子水中,混合均匀备用。按所加试剂总质量计算,氯化钙质量分数约为 2.44%。

(2)预混液配制:分别称取 0.3 g SA 和 0.3 g CS。将 0、50、100、200 mg 和 400 mg LS 分别加入 9.4 mL 去离子水中,超声分散后与 SA、CS 混合,搅拌并振荡至均匀。配液过程中未加入酸。本文所称交联前配液,即本步骤制得、尚未加入氯化钙交联液的 SA/CS/LS 预混液。

(3)凝胶制备:将预混液倒入培养皿铺平,于 4 ℃放置 30 min 辅助脱泡,再于−8 ℃冷冻 30 min 定型;缓慢加入氯化钙交联液并轻微振荡,静置交联 6 h 后,用 10% 乙醇溶液清洗。LS 添加量为 0、50、100、200 mg 和 400 mg 的样品依次记为 SA-CS-LS-0、SA-CS-LS-1、SA-CS-LS-2、SA-CS-LS-3 和 SA-CS-LS-4,配方见表 1。

表 1 复合水凝胶的投料配方

Tab. 1 Initial component amounts for composite hydrogel formulations

Samples	SA/g	CS/g	LS/mg
SA-CS-LS-0	0.3	0.3	0
SA-CS-LS-1	0.3	0.3	50
SA-CS-LS-2	0.3	0.3	100
SA-CS-LS-3	0.3	0.3	200
SA-CS-LS-4	0.3	0.3	400

Notes: Each formulation contains 0.3 g SA, 0.3 g CS, and the specified LS amount, and is prepared with 9.4 mL deionized water.

1.4 测试与表征

(1)微观形貌:将复合水凝胶冷冻干燥后取自然断面,经喷金处理后用导电胶固定于样品台,采用 SEM 在不同放大倍数下观察其内部微观形貌及孔隙结构并采集图像。

(2)化学结构:将冷冻干燥样品进行 FTIR 测试,分析特征吸收及其变化。

(3)力学性能:将样品裁剪为哑铃状,用游标卡尺测量标距段的宽度和厚度;在室温下以 50 mm/min 的速度拉伸至断裂,记录拉伸响应。拉伸强度按最大载荷与初始横截面积之比计算。

(4)加载-卸载测试:以 50 mm/min 的速度拉伸至该批次最大拉伸强度的 80% 后卸载至 0 N,循环 5 次,根据加载-卸载曲线所围成滞后环的面积计算耗散能。

(5)紫外光谱:采用交联前配液进行稀释测试。各配方液先以去离子水稀释至 30 mL,再取 0.3 mL 与 2.7 mL 去离子水混合,置于石英比色皿中测定 200~400 nm 光谱。根据吸光度 A 按 $T=100\times10^{-A}$ 换算表观透过率 T。对 UVB (280~315 nm) 和 UVA (315~400 nm) 分别采用梯形法对 T 随波长的曲线积分,再除以相应波段宽度,得到表观平均透过率;表观平均衰减率为 100% 减去该值。

(6)抑菌性能:以大肠杆菌和金黄色葡萄球菌为受试菌,设置菌液对照组(100 mL TSB)及 0、50、100 mg LS 配方组(50 mL 交联前配液与 50 mL TSB 混合)。各组加入 1 mL 菌液后置于恒温振荡条件下培养,记录 600 nm 处光密度(OD_{600});本文展示 0~10 h 数据。相对生长比 $R=(D_{600,样品}/D_{600,菌液对照})\times100\%$,抑菌率 $I=100\%-R$。$D_{600,样品}$ 和 $D_{600,菌液对照}$ 分别表示同一时间点样品组和无材料菌液对照组用于计算的 OD_{600} 值。当 $R\leq0.01\%$ 时,$I\geq99.99\%$。该指标是基于光密度的生长抑制率。

2 结果与讨论

2.1 SA-CS-LS 复合水凝胶的形成机理

SA-CS-LS 复合水凝胶以 Ca^{2+} 与 SA 羧酸盐基团形成的离子交联网络为骨架,Ca^{2+} 与海藻酸古洛糖醛酸单元形成“蛋盒”结构[2,10]。在此基础上,LS 的酚羟基及其他含氧基团可与 SA、CS 形成氢键;在 CS 氨基质子化的条件下,—NH_3^+ 还可分别与 SA 的—COO^- 和 LS 的—SO_3^- 产生静电作用。LS 引入后可能通过改变非共价连接点和局部链段环境参与网络调控,为力学、抗菌及紫外屏蔽性能的调控提供结构基础。SA、CS 与 LS 及 Ca^{2+} 的可能作用方式如图 1 所示。

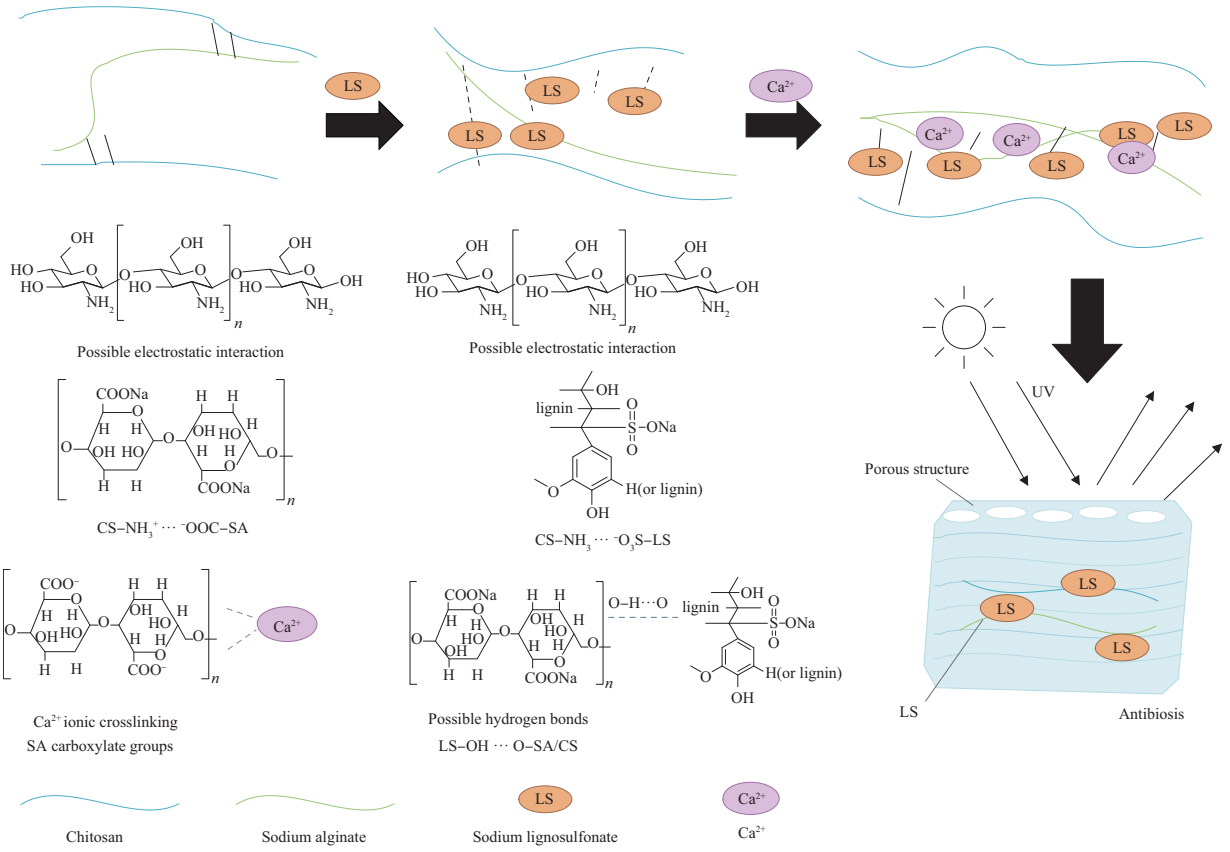


图1 SA/CS/LS复合水凝胶的形成机理示意图

Fig. 1 Schematic illustration of formation mechanism of SA/CS/LS composite hydrogels

图2为LS及SA-CS-LS复合水凝胶的FTIR谱图。由图2可见,SA-CS-LS复合样品保留LS相关吸收特征,在1 000~1 700 cm^{-1}区间呈现谱带形态变化。1 512 cm^{-1}附近的吸收峰可与木质素芳香骨架振动联系,1 000~1 150 cm^{-1}区间包含多糖和LS含氧基团等重叠作用[24]。1 632 cm^{-1}附近同样可能存在多组分吸收叠加,因而不作单一官能团的排他归属。上述变化与组分间非共价相互作用及局部化学环境改变相符,表明LS并非简单分散,而是通过分子间非共价相互作用参与复合网络调控。

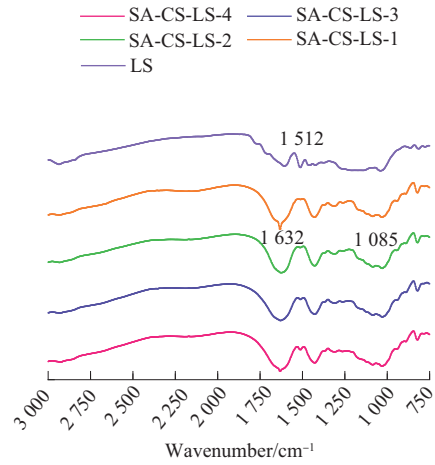


图2 LS及SA-CS-LS复合水凝胶的FTIR谱图

Fig. 2 FTIR spectra of LS and SA-CS-LS composite hydrogels

2.2 SA-CS-LS复合水凝胶的形貌

图3为不同LS添加量的SA-CS-LS复合水凝胶的外观和微观形貌。由图3可见,随着LS添加量的增加,SA-CS-LS凝胶颜色逐渐加深;冷冻干燥后的样品均呈多孔结构,层状形貌逐渐明显,部分区域网络较疏松。较连续的孔壁有利于载荷传递,局部孔壁变薄或结构不均一则可能造成应力集中,与高添加量组复合水凝胶的力学性能下降相联系。

2.3 SA-CS-LS复合水凝胶的力学性能

图4为SA-CS-LS复合水凝胶的力学性能。由图4可见,SA-CS-LS复合水凝胶的拉伸强度随LS添加量的增加而下降。LS添加50 mg和100 mg的SA-CS-LS复合水凝胶拉伸强度分别为0.513 MPa和0.404 MPa,添加200 mg和400 mg的SA-CS-LS复合水凝胶拉伸强度分别为0.262 MPa和0.233 MPa。加载-卸载曲线呈滞后,表明形变过程中存在能量耗散;耗散能也随LS添加量的增加而

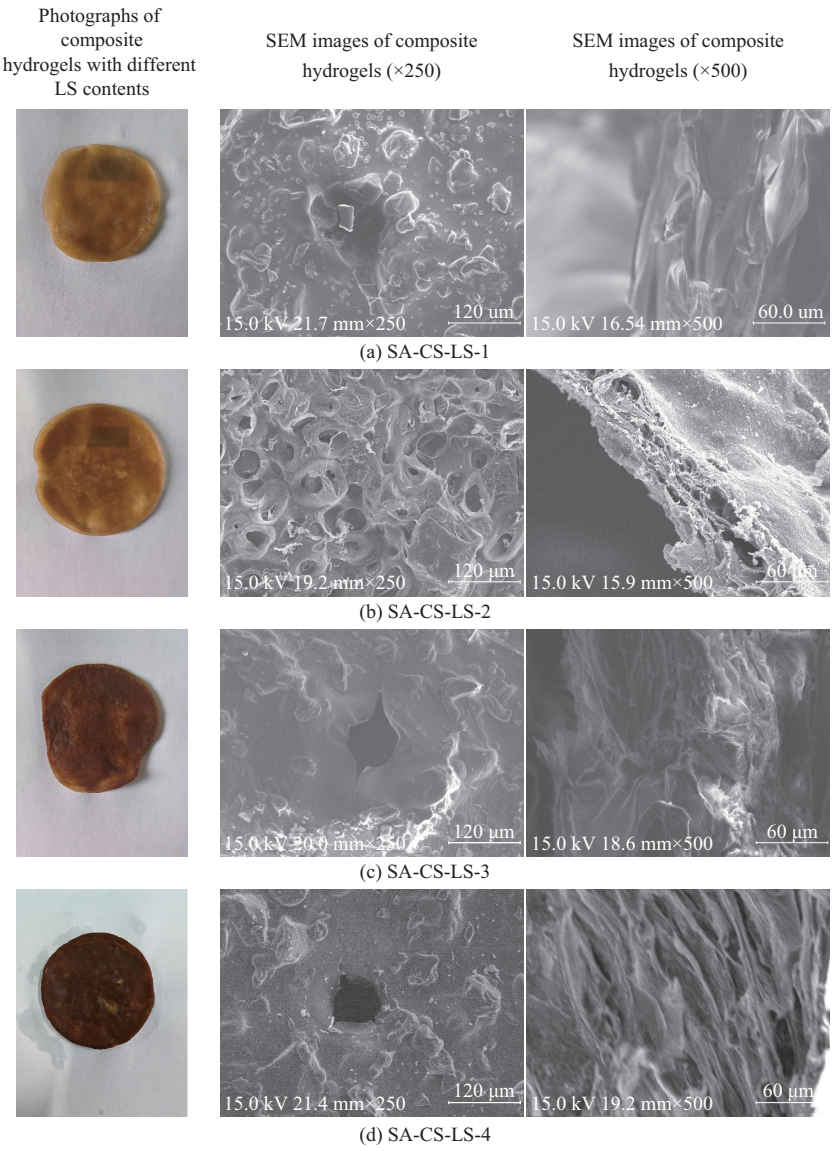


图3 不同LS添加量SA-CS-LS复合水凝胶的宏观透光性与微观形貌

Fig. 3 Macroscopic transparency and microstructure of SA-CS-LS composite hydrogels with different LS contents

降低。低添加量LS可能通过非共价连接改善局部载荷传递;较高添加量引起的链段作用位点竞争、自聚集或分布不均,则可能降低有效连接并引入结构缺陷。

考虑到添加200 mg和400 mg LS的SA-CS-LS复合水凝胶拉伸强度低于添加50 mg和100 mg的SA-CS-LS复合水凝胶,因此后续紫外和抑菌性能分析聚焦于LS添加量为0、50、100 mg的配方,即SA-CS-LS-0、SA-CS-LS-1和SA-CS-LS-2。

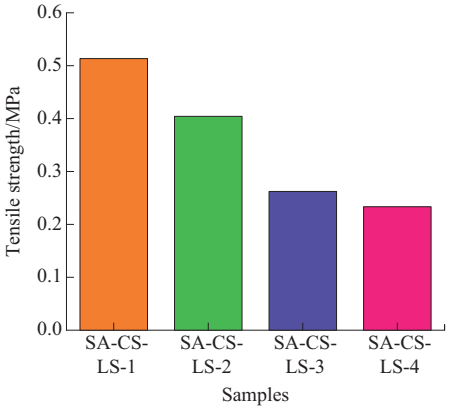
2.4 交联前配液的紫外表观透过率

图5为LS添加量为0、50、100 mg的交联前配液(分别对应SA-CS-LS-0、SA-CS-LS-1和SA-CS-LS-2)经稀释后在200~400 nm范围内的表观透过率曲线,分波段结果见表2。与SA-CS-LS-0配方的稀释液相比,SA-CS-LS-1和SA-CS-LS-2配方的稀释液在UVB区的表观平均透过率降低,SA-CS-LS-2配方的表观平均透过率降至2.79%;其UVA区的表观平均透过率为27.57%,低于SA-CS-LS-0和SA-CS-LS-1配方。SA-CS-LS-1配方的稀释配液在接近400 nm时的透过率高于SA-CS-LS-0配方,因此添加LS后配液表观透过率的降低并非在整个200~400 nm范围内都呈单调变化。

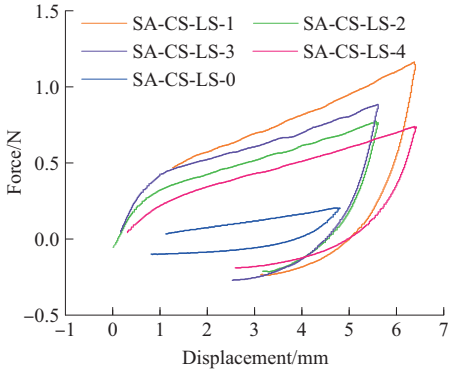
LS的芳香及共轭结构可参与紫外吸收,相关功能也见于木质素基复合薄膜研究[15-18]。本文的剂量变化主要体现在UVB区和部分UVA区,其大小同时受配液浓度、光程及测试基线影响。



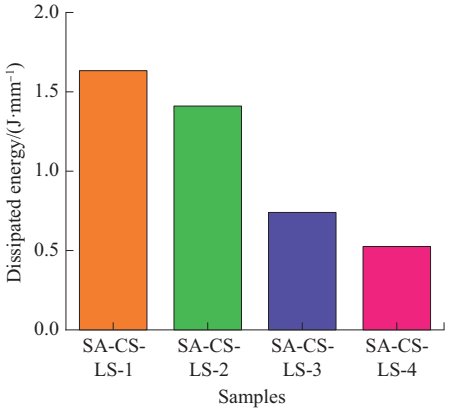
(a) Specimen for mechanical test



(b) Tensile strength of composite hydrogels



(c) Loading-unloading curves of SA-CS-LS-0 to SA-CS-LS-4



(d) Dissipated energy of SA-CS-LS-1 to SA-CS-LS-4

图4 复合水凝胶的力学性能

Fig. 4 Mechanical properties of composite hydrogels

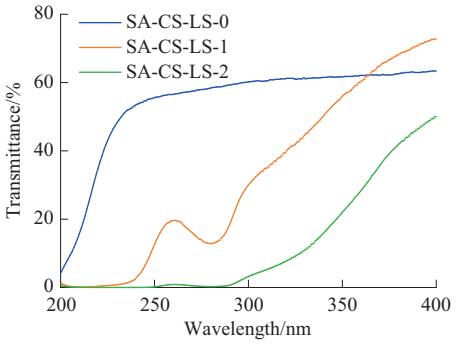


图5 SA-CS-LS-0~SA-CS-LS-2交联前配液经稀释后的表观透过率曲线

Fig. 5 Apparent transmittance spectra of diluted uncrosslinked SA-CS-LS-0 to SA-CS-LS-2 formulation liquids

2.5 交联前配液的OD_{600}计算抑菌表现

图6为LS添加量为0、50、100 mg的三组交联前配液对大肠杆菌和金黄色葡萄球菌的OD_{600}计算抑菌结果，分别对应SA-CS-LS-0、SA-CS-LS-1和SA-CS-LS-2配方。培养2 h时，SA-CS-LS-0配方对大肠杆菌和金黄色葡萄球菌的计算抑菌率分别为82.14%和88.88%，SA-CS-LS-1和SA-CS-LS-2配方的计算抑菌率均接近100%。两种受试菌分别与SA-CS-LS-1和SA-CS-LS-2交联前配液共同培养6 h后，按同一时间点样品组与菌液对照组的OD_{600}比值计算，抑菌率均接近100%。

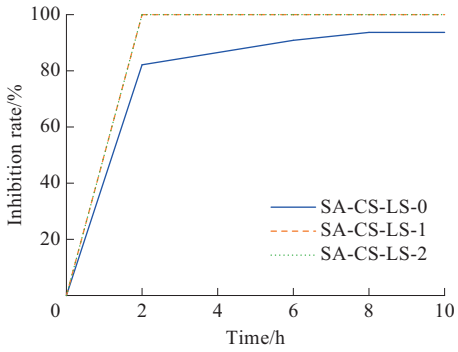
表2 稀释后的交联前配液在UVB和UVA下的表观平均透过率(*T*)及衰减率(*S*)

Tab. 2 Apparent average transmittance (*T*) and attenuation rate (*S*) of diluted solution before crosslinking under UVB and UVA

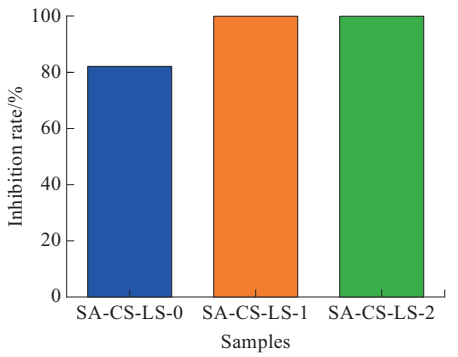
LS dosage/mg	Mean *T* at UVB/%	Mean *S* at UVB/%	Mean *T* at UVA/%	Mean *S* at UVA/%
0	59.86	40.14	62.02	37.98
50	25.92	74.08	57.84	42.16
100	2.79	97.21	27.57	72.43

Notes: *T* is apparent mean transmittance calculated over the specified wavelength band; *S*=100−*T*; UVB is 280−315 nm mid-wave ultraviolet light; UVA is 315−400 nm long-wave ultraviolet light.

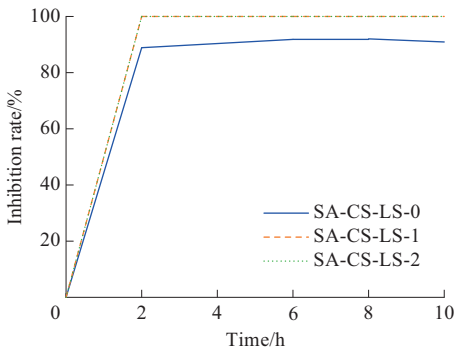
CS及木质素材料的抑菌活性已有报道[19−20]。LS引入后，体系组成、可接触基团及材料与菌体的界面作用均可能发生变化，从而影响生长抑制。与SA-CS-LS-1相比，SA-CS-LS-2的拉伸强度有所降低，但其配液在UVA和UVB波段的表观平均透过率更低，



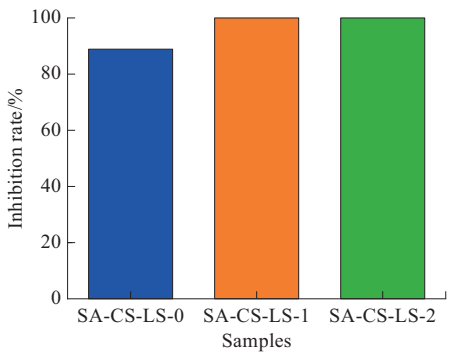
(a) Inhibition curves against Escherichia coli



(b) 2 h inhibition rate against Escherichia coli



(c) Inhibition curves against Staphylococcus aureus



(d) 2 h inhibition rate against Staphylococcus aureus

图6 基于OD_{600}计算的抑菌率时间曲线及2 h抑菌率

Fig. 6 Time courses of OD_{600}-derived inhibition rates and inhibition rates at 2 h

两组的OD_{600}计算抑菌率接近。因此,SA-CS-LS-2可作为兼顾力学、紫外及抑菌表现的候选配方。

3 结论

采用Ca^{2+}离子交联制备了SA/CS/LS复合水凝胶。LS添加量的增加伴随层状形貌增强和局部网络疏松,当LS添加量由50 mg增加到400 mg时,SA-CS-LS复合水凝胶的拉伸强度由0.513 MPa降至0.233 MPa,耗散能同步下降。对LS添加量为0、50、100 mg的配方(SA-CS-LS-0至SA-CS-LS-2)的后续测试表明,SA-CS-LS-2配方所制得的凝胶具有0.404 MPa的拉伸强度,其交联前配液稀释液在UVB和UVA波段的表观平均透过率分别为2.79%和27.57%;两种受试菌分别与SA-CS-LS-1和SA-CS-LS-2交联前配液共同培养6 h后,OD_{600}计算抑菌率均不低于99.99%。上述结果说明,LS可用于调节SA/CS复合体系的结构及力学与功能平衡,为抗菌、紫外防护型外用眼贴基材的配方设计提供参考。

参 考 文 献

[1] 吴晓娜,汪宜宇,赵凯. MXene基复合水凝胶在修复感染创面中的研究进展[J].复合材料学报,2024,41(7):3 427–3 441.
WU Xiaona, WANG Yiyu, ZHAO Kai. MXene and its composite hydrogel application in infective wound healing[J]. Acta Materiae Compositae Sinica,2024,41(7):3 427–3 441.

[2] CAO Y, CONG H L, YU B, et al. A review on the synthesis and development of alginate hydrogels for wound therapy[J]. Journal of Materials Chemistry B,2023,11(13):2 801–2 829.

[3] KRUTMANN J, BÉHAR-COHEN F, BAILLET G, et al. Towards standardization of UV eye protection: What can be learned from photodermatology? [J]. Photodermatology, Photoimmunology & Photomedicine,2014,30(2/3):128–136.

[4] PITTAYAPRUEK P, MEEPHANSAN J, PRAPAPAN O, et al. Role of matrix metalloproteinases in photoaging and photocarcinogenesis[J]. International Journal of Molecular Sciences, 2016, 17 (6). DOI:10.3390/ijms17060868.

[5] MAJDI M, MILANI B Y, MOVAHEDAN A, et al. The role of ultraviolet radiation in the ocular system of mammals[J]. Photonics,2014,1(4):347–368.

[6] 韦嘉盛,戴磊,贺瓶.基于纤维素及其衍生物的凝胶材料设计[J].复合材料学报,2022,39(7):3 084–3 103.
WEI Jiasheng, DAI Lei, HE Ping. Design of gel materials with cellulose and its derivatives[J]. Acta Materiae Compositae Sinica, 2022,39(7):3 084–3 103.

[7] 杨明琰,陈欣玥,张笑,等.双醛纤维素/聚乙烯醇复合水凝胶的制备及其性能[J].复合材料学报,2022,39(10):4 889–4 897.
YANG Mingyan, CHEN Xinyue, ZHANG Xiao, et al. Preparation and properties of dialdehyde cellulose/polyvinyl alcohol composite hydrogel[J]. Acta Materiae Compositae Sinica,2022,39(10):4 889–4 897.

[8] 耿志杰,于珊,曾志文,等.壳聚糖/海藻酸钠自修复水凝胶的制备与性能[J].暨南大学学报(自然科学与医学版),2022,43(3):322–331.
GENG Zhijie, YU Shan, ZENG Zhiwen, et al. Preparation and characterization of self-healing hydrogel based on chitosan/sodium alginate[J]. Journal of Jinan University (Natural Science & Medicine Edition),2022,43(3):322–331.

[9] 孙士儒,刘阳,王景辉,等.具有不同拓扑结构的海藻酸钠-明胶复合水凝胶的3D打印制备及其性能[J].复合材料学报,2022,39(8):4 049–4 056.
SUN Shiru, LIU Yang, WANG Jinghui, et al. Preparation and properties of sodium alginate-gelatin composite hydrogels with different topological structures by 3D printing[J]. Acta Materiae Compositae Sinica,2022,39(8):4 049–4 056.

[10] SINGH A K, PRAMANIK K. Fabrication and investigation of physicochemical and biological properties of 3D printed sodium alginate-chitosan blend polyelectrolyte complex scaffold for bone tissue engineering application[J]. Journal of Applied Polymer Science,2023,140(12). DOI:10.1002/app.53642.

[11] MAO G Z, TIAN S Y, SHI Y X, et al. Preparation and evaluation of a novel alginate-arginine-zinc ion hydrogel film for skin wound healing[J]. Carbohydrate Polymers, 2023, 311. DOI: 10.1016/j.carbpol.2023.120757.

[12] ZHANG H J, WANG X, HUANG H X, et al. Nanocomposite interpenetrating hydrogels with high toughness and good self-recovery[J]. Colloid and Polymer Science, 2019, 297(6):821–830.

[13] 姜波,金永灿.基于木质素分子结构特性的功能材料研究进展[J].复合材料学报,2022,39(7):3 059–3 083.
JIANG Bo, JIN Yongcan. Research progress of lignin functional materials based on its structural properties[J]. Acta Materiae Compositae Sinica,2022,39(7):3 059–3 083.

[14] 盖晓倩,李雨,雷同,等.木质素基功能材料在阻隔包装纸中的应用研究进展[J].复合材料学报,2024,41(8):3 935–3 949.
GAI Xiaoqian, LI Yu, LEI Tong, et al. Research progress on the application of lignin-based functional materials in barrier packaging paper[J]. Acta Materiae Compositae Sinica, 2024, 41(8):3 935–3 949.

[15] ZHANG W B, ZHANG Y, LIANG H Y, et al. High bio-content castor oil based waterborne polyurethane/sodium lignosulfonate composites for environmental friendly UV absorption application[J]. Industrial Crops and Products, 2019, 142. DOI: 10.1016/j.indcrop.2019.111836.

[16] HE Y, YE H C, YOU T T, et al. Sustainable and multifunctional cellulose-lignin films with excellent antibacterial and UV-shielding for active food packaging[J]. Food Hydrocolloids,2023,137. DOI:10.1016/j.foodhyd.2022.108355.

[17] GUO Y L, YOU Y, GUO G, et al. Facile preparation of cellulose/lignosulfonate derivatives composite films with high UV-shielding and gas barrier properties[J]. International Journal of Biological Macromolecules, 2023, 237. DOI: 10.1016/j.ijbiomac.2023.124218.

[18] LI X R, LIU Y, REN X H. Transparent and ultra-tough PVA/alkaline lignin films with UV shielding and antibacterial functions[J]. International Journal of Biological Macromolecules, 2022, 216:86–94.

[19] KOU S, PETERS L, MUCALO M. Chitosan:A review of molecular structure, bioactivities and interactions with the human body and micro-organisms[J]. Carbohydrate Polymers, 2022, 282. DOI:10.1016/j.carbpol.2022.119132.

[20] MORENA A G, BASSEGODA A, NATAN M, et al. Antibacterial properties and mechanisms of action of sonoenzymatically synthesized lignin-based nanoparticles[J]. ACS Applied Materials & Interfaces,2022,14(33):37 270–37 279.

[21] SUN M Y, LIU N, NI S Z, et al. Enhanced strength, antioxidant and barrier properties of chitosan-based film by bentonite and lignosulfonate[J]. Food Packaging and Shelf Life, 2024, 42. DOI:10.1016/j.fpsl.2024.101246.

[22] VAN PHUC N, THANG N H, LE ANH KHOA T. Evaluation on effects of chitosan derived from shrimp shells on engineering properties, antioxidant, antibacterial, and microstructural characteristics of chitosan-alginate-carrageenan-based hydrogels[J]. Journal of Applied Polymer Science, 2025, 142(32). DOI:10.1002/app.57278.

[23] ZHANG X R, YANG L F, WANG W C, et al. Sodium alginate/sodium lignosulfonate hydrogel based on inert Ca^{2+} activation for water conservation and growth promotion[J]. Environmental Research, 2024, 246. DOI:10.1016/j.envres.2024.118144.

[24] KARPUKHINA E A, VOLKOV D S, PROSKURNIN M A. Quantification of lignosulfonates and humic components in mixtures by ATR FTIR spectroscopy[J]. Agronomy, 2023, 13(4). DOI:10.3390/agronomy13041141.